EEET ECOLOGICAL ENGINEERING & ENVIRONMENTAL TECHNOLOGY

Ecological Engineering & Environmental Technology 2024, 25(3), 287–296
https://doi.org/10.12912/27197050/178403
ISSN 2719–7050, License CC-BY 4.0

Received: 2023.12.10
Accepted: 2024.01.08
Published: 2024.01.26

Characterization of Metallic Gold Nanoparticles in a Colloidal State by Artificial Vision

Hipólito Carbajal-Morán[1], Carlos A. Galván-Maldonado[1], Javier F. Márquez-Camarena[1*]

[1] Universidad Nacional de Huancavelica, Instituto de Investigación de Ciencias de Ingeniería, Facultad de Ingeniería Electrónica-Sistemas, Jr. La Mar 755, Pampas 09156, Huancavelica, Perú

* Corresponding author's e-mail: javier.marquez@unh.edu.pe

ABSTRACT

Gold nanoparticles in their colloidal state have different colors, and the equipment for their characterization, such as UV-Vis spectrophotometers, scanning electron microscopy (SEM), and transmission electron microscopy (TEM), has high costs. The research aimed to characterize metallic gold nanoparticles by artificial vision based on the color of the samples in the colloidal state. The sensor used for the sampling was a 50 MP triple-lens camera with the optical image stabilization (OIS) of a smartphone. The Vision Acquisition and Vision Assistant blocks in the NI LabVIEW platform were used to implement an artificial vision device. The camera interface was used to identify the color of each of the 10 samples of colloidal gold nanoparticles produced by the YAG laser and chemical reduction in 15 ml of deionized water. The characterization consisted of the determination of the size and concentration of the gold nanoparticles based on their color, which ranged from pink to red wine. As a result, the artificial vision device adequately identified the color of the metallic gold nanoparticles in a colloidal state with a certainty of more than 95%, allowing the nanoparticles to be adequately characterized. Therefore, it is concluded that artificial vision adequately characterized gold nanoparticles' wavelength, absorbance, diameter, and concentration.

Keywords: gold metal nanoparticles, color characterization, artificial vision, spectrophotometry, optical microscopy.

INTRODUCTION

Metal nanoparticles (NPs) are particles less than 100 nanometers in diameter that have unique properties that differentiate them from macroscopic-scale materials. These properties make them attractive for a wide range of applications, such as biomedicine (Paramasivam et al., 2024), electronics (Weichelt et al., 2019), catalysis, and optics such as in the treatment of contaminated water (Kumari et al., 2024).

Gold nanoparticles (AuNPs) are a type of metallic NP that have been widely studied due to their unique optical properties (Liu et al., 2021). AuNPs are highly dispersible in water and exhibit a characteristic red color variant according to their size and shape. This property has made them a promising material for applications in bioimaging, biosensing, and photodynamic therapy (Hua et al., 2021).

Characterization of AuNPs is critical for the development of successful applications. The properties of AuNPs, such as their size, shape, size distribution, and aggregation state, can significantly affect their performance in a given application. Traditionally, AuNPs have been characterized using laboratory techniques, such as optical spectroscopy, electron microscopy, and X-ray diffraction. These techniques are accurate but are laborious and expensive.

In recent years, artificial vision (AV), part of artificial intelligence, has become a tool that makes color, image, and morphology detection possible (Balarezo et al., 2022; Serafino et al., 2020). AV can automate image analysis (Montalvan et al., 2022) and provide quantitative and qualitative information about image properties.

LabVIEW is a software tool designed for the development of applications intended for monitoring, control, and design using graphical programming (Korgin et al., 2019); its distinctive feature lies in providing a user-friendly environment, by adopting a graphical approach, LabVIEW simplifies the creation of complex applications by replacing extensive lines of code with an intuitive visual environment (Sivaranjani et al., 2021). LabVIEW as a virtual instrument mimicking instrument simulation software can display real-time object detectors with IGUI design (Fawwaz et al., 2020). LabVIEW has modules developed for AV, among these modules are Vision Acquisition and Vision Assistant (NI, 2023); in addition, it has great compatibility with other programs, cameras, and vision systems.

Early applications of AV focused on object detection and counting, nowadays, AV is used to characterize a wide range of object properties, such as size, shape, size distribution, and aggregation states (Wisultschew et al., 2019). With AV, image analysis can be automated, which reduces the time and effort required for characterization; it can be adapted to different sample types and experimental conditions. It requires a significant amount of training data to achieve optimal performance (Arsalane et al., 2020). The AV method of image analysis uses image processing techniques to extract information about the properties of objects such as AuNPs found in a colloidal state, this method includes edge detection, image segmentation, and color analysis (Ganchovska & Krasteva, 2022).

The application of AV in the characterization of aqueous substances is achievable by color detection; as the study of Ordoñez-Avila et al. (2022), where they implemented controllers to detect color change by AV in the formation of ice in an evaporator, once the desired color is obtained, the controller sends a shutdown signal; with which obtained water of a defined color. On the other hand, nanoparticles have been the subject of continuous research and development. In the study by Nag et al. (2020), the capabilities of VA for size and shape determination of metal nanoparticles in colloidal solutions were explored; the results highlighted the effectiveness of this methodology in overcoming the challenges associated with size and morphology variability, thus laying the foundation for this research.

In this context, VA is an approach to overcome the cost and speed limitations in characterizing AuNPs in a colloidal state, by applying advanced image processing algorithms implemented in LabVIEW using Vision Acquisition and Vision Assistant (Issa et al., 2019). VA enables a quantitative and qualitative evaluation of the properties of NPs in colloidal solutions. This methodology is presented as an innovative tool for the rapid characterization of AuNPs in colloidal environments with color sorting.

MATERIALS AND METHODS

Gold nanoparticle synthesis

The synthesis of AuNPs was carried out by the laser ablation method, a process that uses a laser, with which it was ablated on a solid gold plate of 10×15 mm with a thickness of 1 mm inside ultrapure deionized water. This method allowed the production of AuNPs dispersed in solution, with significant control over their size and characteristics. A high-energy pulsed Nd: YAG (Neodymium: Yttrium-Aluminum-Garnet) laser was used, emitting short 6 ns and powerful pulses up to 450 mJ/pulse for different wavelengths (Quantel, 2019).

The laser beam was focused on the Au solid plate, located 100 mm away from a convex lens (Figure 1). The laser energy is absorbed by the Au, which is immersed in water, generating plasma at this solid-liquid interface. The interaction between the laser and the gold target produces a hot, highly energetic plasma on the surface of the material. The plasma reaches extremely high temperatures (Torrisi et al., 2020), leading to vaporization and the formation of a plasma plume. The laser parameters, such as pulse energy and repetition rate, as well as the focal length and duration of the ablation process, were tuned to produce AuNPs with different characteristics.

The ablation of the Au target generates microscopic fragments and NPs in the plasma plume; the laser energy breaks the atomic bonds, generating ions and atoms that condense and form NPs during the expansion and cooling of the plasma. These generated Au are dispersed in ultrapure water and stabilized in the form of colloids with characteristic colors according to their size and concentration. Analyses are performed to characterize the properties of the AuNPs synthesized by the laser ablation method; such as size, shape, and concentration.

As shown in Figure 2, also, AuNPs are produced by the size-controlled chemical reduction method (Zhou et al., 2023); employing an aqueous solution of gold chloride ($AuCl_4$) as a precursor and a reducing agent, such as sodium borohydride ($NaBH_4$), under controlled conditions of temperature and agitation (Iqbal et al., 2016).

The formation of AuNPs by both laser ablation and chemical reduction methods was confirmed by UV–Vis spectroscopy using AvaSpec-ULS2048x64-EVO equipment (Avantes, 2018).

Colloidal solutions preparation

The colloidal solutions of the synthesized AuNPs were dispersed using an ultrasound (US) system at 40 kHz (Carbajal-Morán et al., 2022), to ensure a homogeneous distribution (Figure 3). The concentrations of the colloidal solutions were adjusted to encompass a suitable range of sizes and optical densities.

Once the AuNPs were homogenized in a colloidal state, the samples were placed in 5 ml transparent glass vials to be characterized by artificial vision.

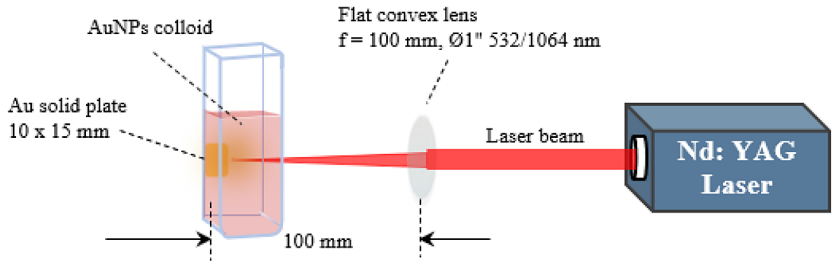

Figure 1. Diagram of colloidal AuNPs generation with Nd: YAG laser

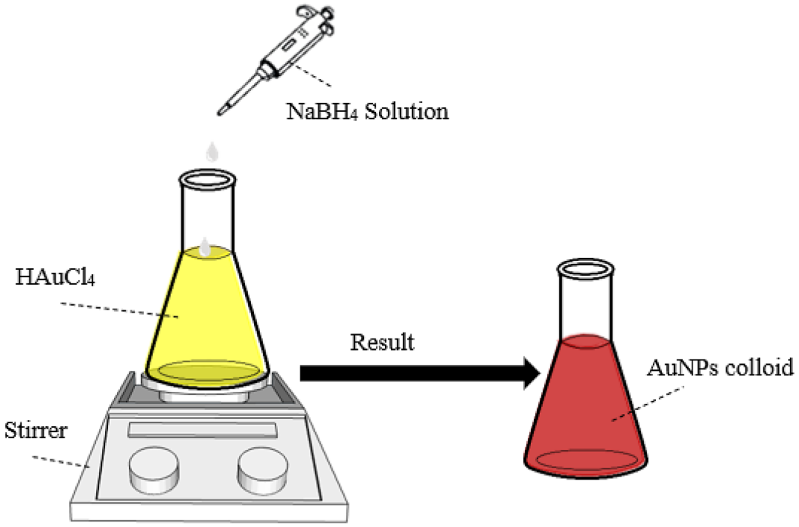

Figure 2. Diagram of colloidal AuNPs generation with $NaBH_4$ as reducing agent

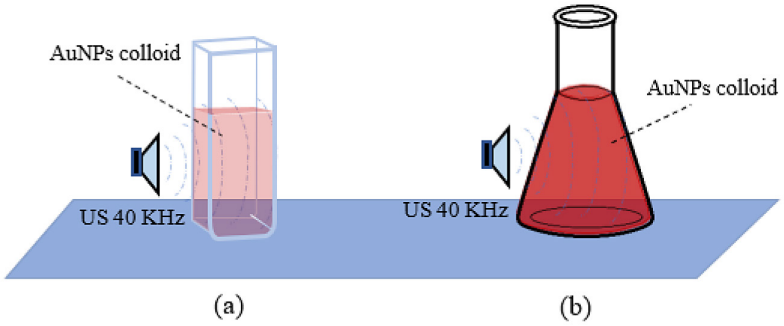

Figure 3. Homogenization of colloidal AuNPs with 40 KHz US, a) AuNPs generated with Nd: YAG laser, and b) AuNPs generated with $NaBH_4$ as reducing agent

Artificial vision system development

Figure 4 presents the implementation diagram of an AV system using LabVIEW as the development platform, Vision Acquisition Software (Zhang et al., 2019) was used as the controller to acquire, visualize, and save images from the 50 MP OIS smartphone triple camera device OIS using USB communication, through the freely distributed DroidCamApp interface (Ajey et al., 2023). To then be characterized by presenting the maximum peak absorbance as a function of the wavelength of the spectrum; with which the diameters and concentrations of the AuNPs of the samples were determined.

The Vision Acquisition block was configured to acquire the image of the AuNPs in video mode with a resolution of 29.97 fps (Figure 5).

On the other hand, the Vision Assistant block (Figure 6) contains a training interface for the classification of AuNPs colloids by color. The characteristic colors of most commonly used AuNPs were considered (Mohandas, 2020; Strem Chemicals, 2011; Torskal Nanoscience, 2022); these being spherical with diameters of 5, 10, 15, 15, 20, 25, 25, 50, 50, 60, 60, 75, 90, and 100 nm.

Figure 7 shows the selection of the control by classes with color classification of the AuNPs and indicators for access from LabVIEW.

From the classification and characterization diagram of the AuNPs colloid samples developed in LabVIEW (Figure 8), it was possible to plot the maximum peak absorbance as a function of its wavelength, by reading the corresponding *.csv file that was displayed on the Graph element of LabVIEW.

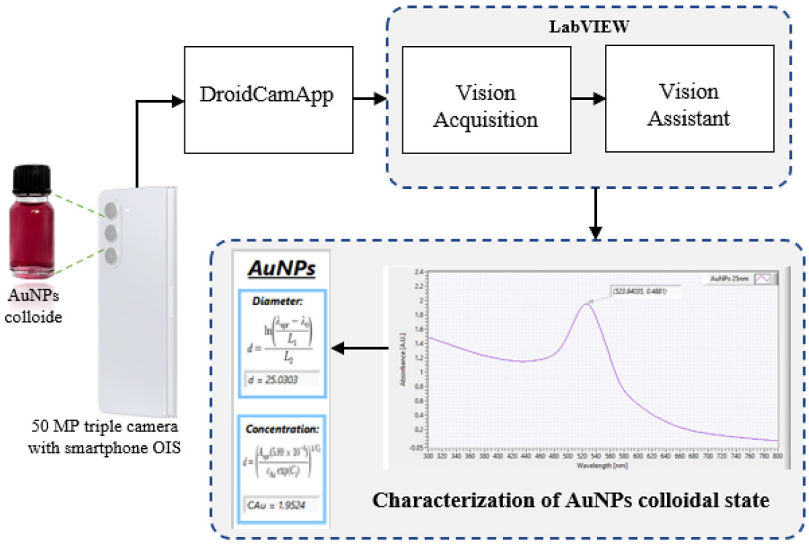

Figure 4. Characterization diagram of AuNPs in a colloidal state by artificial vision

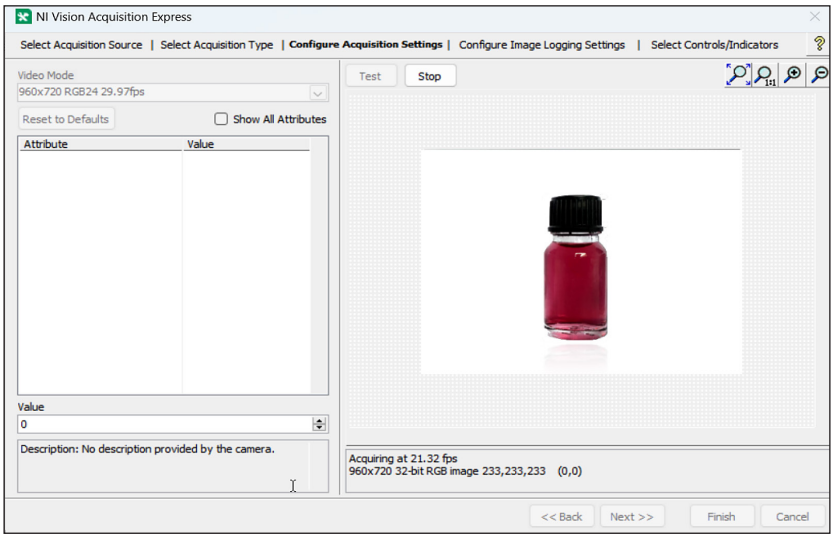

Figure 5. Vision Acquisition block configuration at 29.9 fps resolution

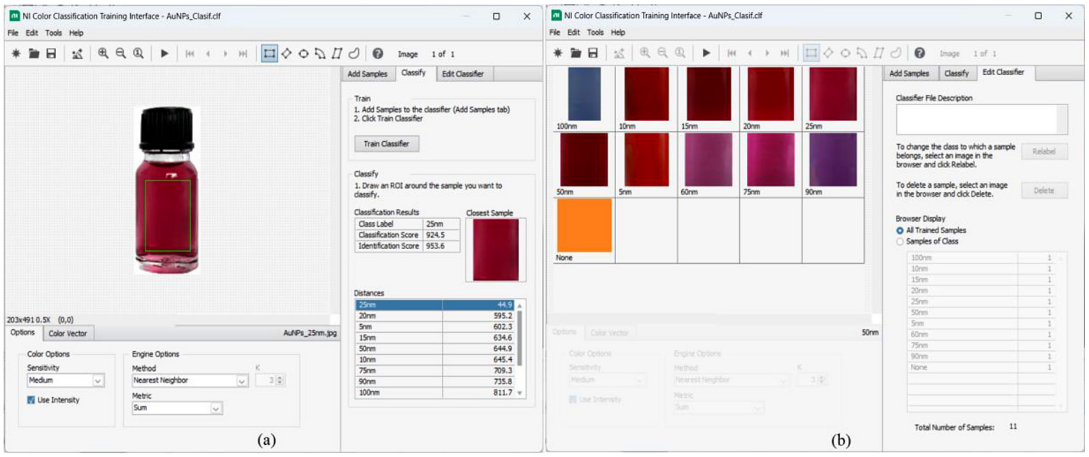

Figure 6. (a) Classification of AuNPs colloid samples and (b) Training interface for color classification of AuNPs colloid samples

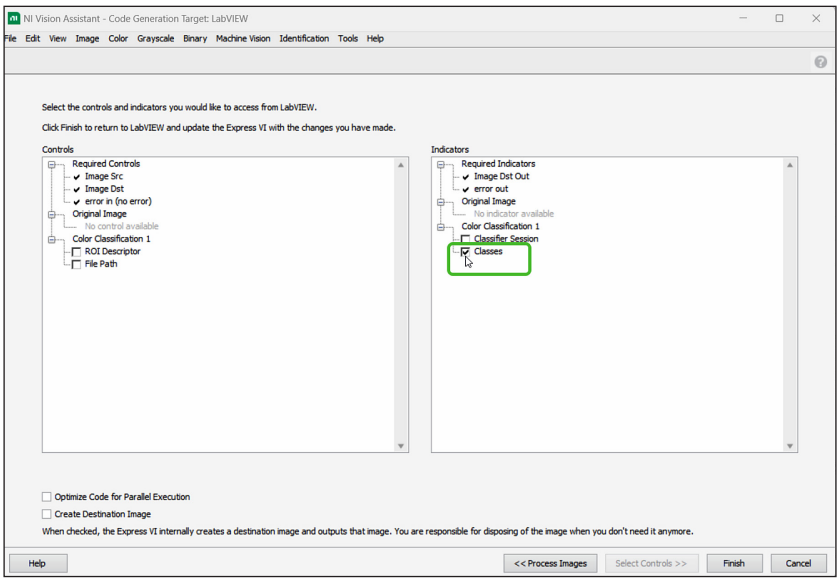

Figure 7. Selection of class-based control for access from LabVIEW

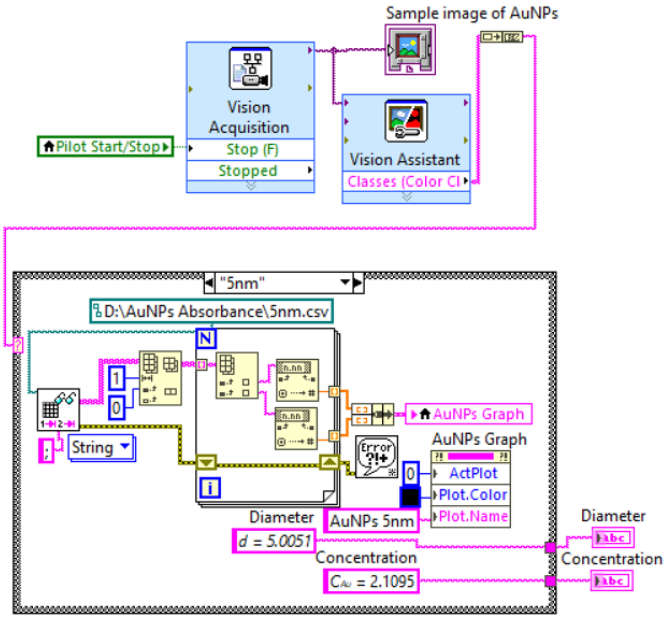

Figure 8. Classification and characterization diagram of AuNPs colloid samples in LabVIEW

The sample diameters of the AuNPs were calculated with Equation 1 as a function of the absorbance of the AuNPs (Haiss et al., 2007); considering the peak absorbance wavelength (λ_{spr}) with $\lambda_0 = 512$ nm, $L_1 = 6.530$ and $L_2 = 0.0216$.

$$d = \frac{\ln\left(\frac{\lambda_{spr}-\lambda_0}{L_1}\right)}{L_2} \quad (1)$$

With "*d*" obtained in Eq. 1, the concentration of AuNPs was calculated, using Equation 2:

$$C_{Au} = \left(\frac{A_{spr}(5.89 \cdot 10^{-6})}{\exp(C_1)}\right) \cdot d^{-C_2} \quad (2)$$

where: A_{spr} – represents the absorbance at peak plasmon resonance, C_{Au} – concentration of nanoparticles mg/l, with experimental values $C_1 = -4.750$ and $C_2 = 0.314$ (Haiss et al., 2007).

From the front panel of the artificial vision system developed in LabVIEW, presented in Figure 9, it was possible to characterize the samples of AuNPs in a colloidal state; showing the signal of the observance, the diameter, and the concentration of NPs, calculated with equations 1 and 2.

RESULTS AND DISCUSSION

With the artificial vision system implemented in LabVIEW, it was possible to characterize the AuNPs that were in the colloidal state with spherical shapes, with diameters close to 5, 10, 15, 20, 25, 50, 50, 60, 75, 90 and 100 nm, whose results are shown from (a) to (j) in Figure 10 corresponding to each diameter.

Based on the standard samples after training, the characterizations of the AuNPs were performed, determining the average wavelength, diameter, absorbance, and concentration of the NPs, which are presented in Table 1.

In Figure 11, the wavelength of the AuNPs in the standard samples was compared with the wavelengths obtained with AV implemented in LabVIEW. From the results, it is observed that the p-value is 0.338, which is higher than 0.05, so it is determined that the wavelength measured with the AV of the AuNPs is practically equal to the wavelength established in the standard samples.

Likewise, when comparing the diameters of the AuNPs measured concerning the standard samples using AV implemented in LabVIEW, a p-value of 0.879 was obtained, which indicates that the measured diameters fit with high precision to those established (Figure 12).

On the other hand, Figure 13 shows the relationship of the measured diameters with the absorbances and concentrations of AuNPs, where the measured peak plasmon resonance absorbance of the different AuNPs samples as a function of their diameter "*d*" can be represented by $A_{spr} = -0.0144d + 2.2852$, for an $R^2 = 0.962$. While the concentration of the AuNPs is represented by $C_{Au} = -0.0067d + 0.7321$, for an $R^2 = 0.911$.

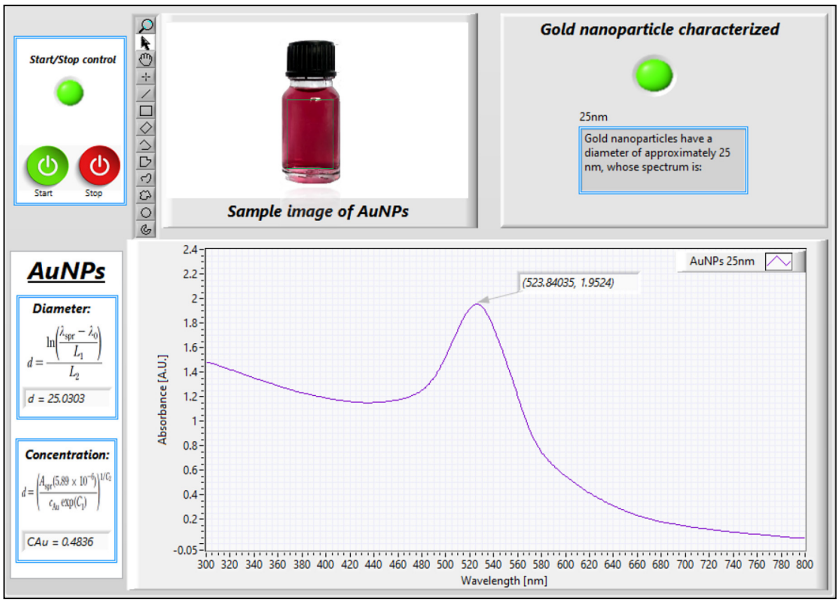

Figure 9. LabVIEW front panel of the artificial vision system for the characterization of AuNPs in colloidal state

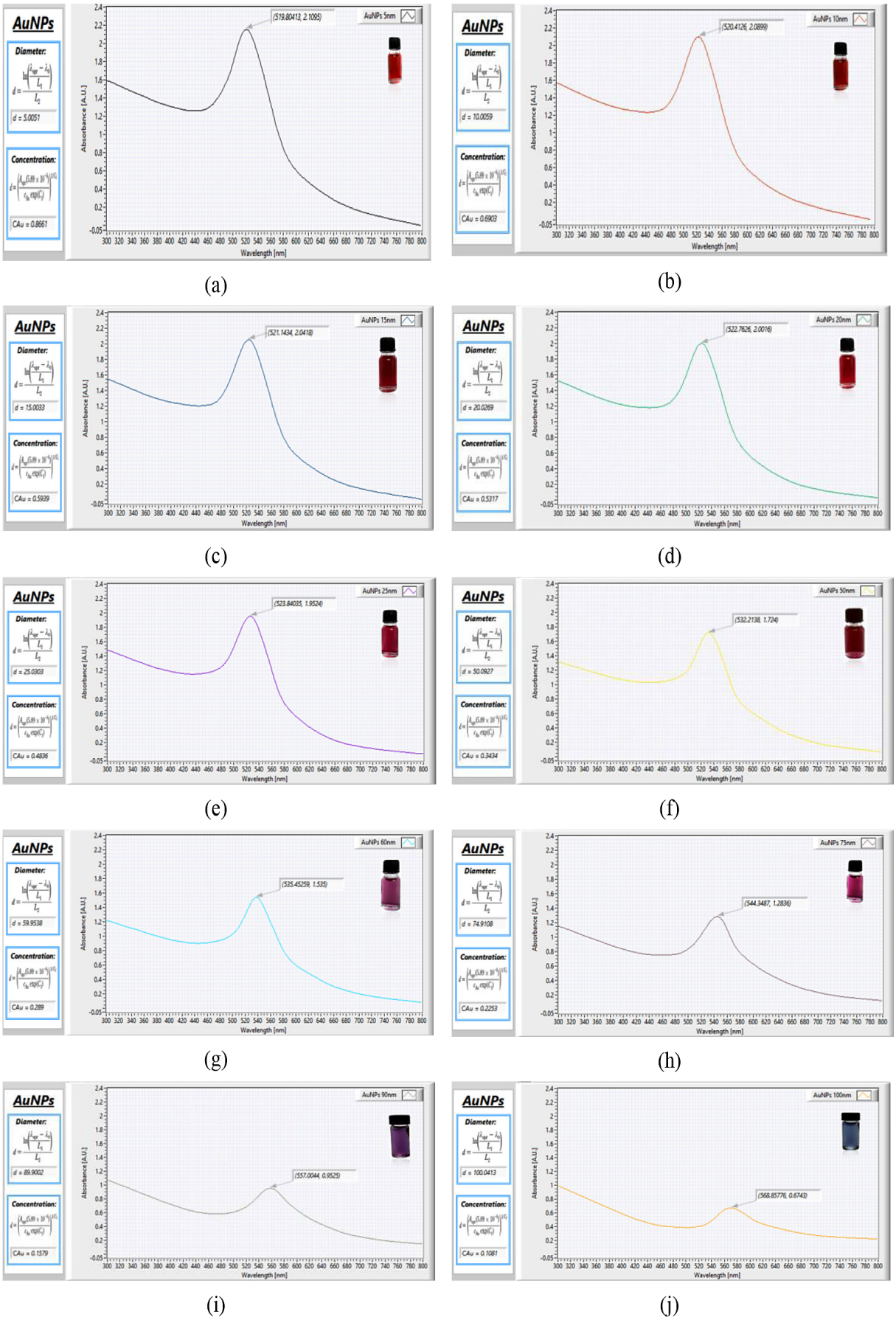

Figure 10. Characterization result of AuNPs in a colloidal state by artificial vision implemented in LabVIEW

Table 1. AuNPS pattern sample and average values of the AuNPs characterization

N°	AuNPs pattern sample		Average values of the AuNPs characterization			
	Diameter (nm)	Wavelength (nm)	Measured wavelength (nm)	Measured diameter (nm)	Absorbance (A.U.)	Concentration (mg/L)
1	5	519.2747	519.8041	5.0051	2.1095	0.8661
2	10	520.1044	520.4126	10.0059	2.0899	0.6903
3	15	521.0287	521.1434	15.0033	2.0418	0.5939
4	20	522.0584	522.7626	20.0270	2.0016	0.5317
5	25	523.2055	523.8404	25.0303	1.9524	0.4836
6	50	531.2288	532.2138	50.0927	1.7240	0.3434
7	60	535.8649	535.4526	59.9538	1.5350	0.2890
8	75	544.9967	544.3487	74.9108	1.2836	0.2253
9	90	557.6228	557.0044	89.9002	0.9525	0.1579
10	100	568.6225	568.8578	100.0414	0.6743	0.1081

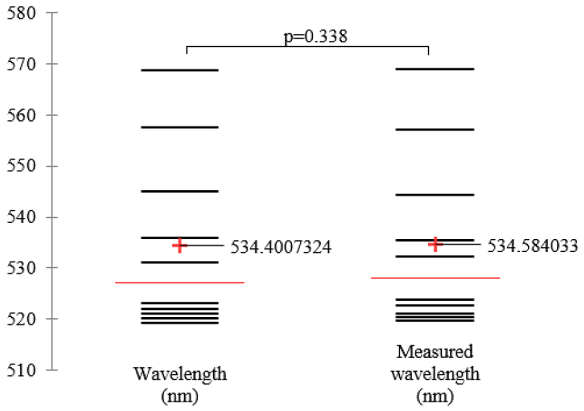

Figure 11. Strip plots of the wavelength of AuNPs measured about the standard sample

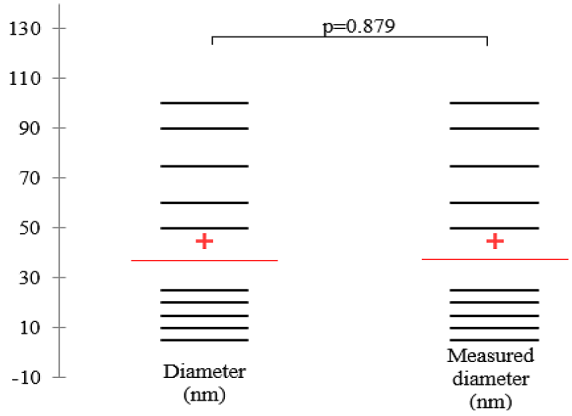

Figure 12. Strip plots of the AuNPs diameter measured about the standard sample

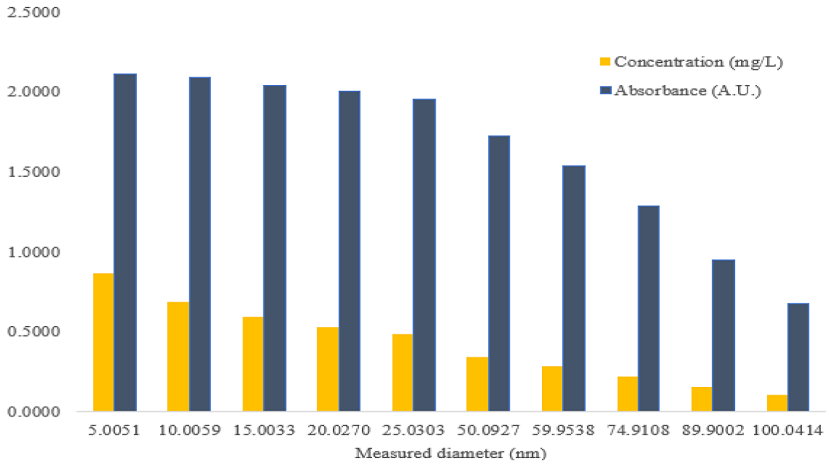

Figure 13. The ratio of measured diameter to absorbance and concentration of AuNPs

CONCLUSIONS

The configuration of the Vision Acquisition block to obtain high-quality images and the training of color classification in LabVIEW's Vision Assistant were performed so that it could be sensitive to the variation of the characteristic colors of AuNPs, according to their diameter and concentration in liquid media.

The implementation of AV in LabVIEW enabled accurate determination of the diameter of colloidal AuNPs. The ability to analyze images at different scales and the optimization of class-based algorithms for color classification were key to obtaining detailed and reliable measurements of the diameter of NPs that were in the range of approximately 5–100 nm. Also, a clear relationship was established between the wavelength of the incident light and the absorbance of the AuNPs. AV in LabVIEW facilitated the identification of spectral patterns, which contributed to understanding how the concentration of NPs affects the absorbance at different wavelengths.

With the implementation of Equation 2 (Haiss et al., 2007) on the LabVIEW platform, the concentration of colloidal AuNPs was calculated. This analysis is important to understand how changes in concentration can affect the optical response, which is valuable information for applications in sensors and optoelectronic devices.

The results obtained using AV implemented in LabVIEW were validated against conventional UV–Vis characterization methods. The consistency between the results demonstrates the reliability of the implemented system and its ability to provide accurate and comparable data at a low cost.

Acknowledgements

This work was possible thanks to the support of the specialized laboratory of optics and lasers of the electronic engineering career of the National University of Huancavelica.

REFERENCES

1. Ajey, H., Mardiati, R., Kamelia, L. 2023. Automatic presence system with face recognition based smartphone camera using the haar cascade method. EasyChair Preprint No. 10527.
2. Arsalane, A., Klilou, A., Barbri, N.E., Tabyaoui, A. 2020. Artificial vision and embedded systems as alternative tools for evaluating beef meat freshness. IEEE 6th International Conference on Optimization and Applications (ICOA), 1–6. https://doi.org/10.1109/ICOA49421.2020.9094503
3. Avantes. 2018. Espectrómetro UV-Vis-NIR - Ava Spec-ULS2048x64-EVO. https://www.medicalexpo.com/prod/avantes/product-104219-950813.html
4. Balarezo, S., Arias, X., Espín, K., Aquino, M., Novillo, G. 2022. Simulation system of a tomato sorting process using artificial vision BT - emerging research in intelligent systems. M. Botto-Tobar, H. Cruz, A. Díaz Cadena, & B. Durakovic (Eds.), Springer International Publishing, pp. 135–146.
5. Carbajal-Morán, H., Rivera-Esteban, J.M., Aldama-Reyna, C.W., Mejía-Uriarte, E.V. 2022. Functionalization of gold nanoparticles for the detection of heavy metals in contaminated water samples in the province of Tayacaja. Journal of Ecological Engineering, 23(9), 88–99. https://doi.org/10.12911/22998993/151745
6. Fawwaz, F., Dunggio, B., Wulandari, P., Rahyadi, I., Astharini, D. 2020. Vision application of LabVIEW: IGUI for face and pattern detection in real time. 2020 International Conference on Information Management and Technology (ICIMTech), 438–442. https://doi.org/10.1109/ICIMTech50083.2020.9211282
7. Ganchovska, V., Krasteva, I. 2022. Converting color to grayscale image using LabVIEW. International Conference Automatics and Informatics (ICAI), 320–323. https://doi.org/10.1109/ICAI55857.2022.9960062
8. Haiss, W., Thanh, N.T.K., Aveyard, J., Fernig, D.G. 2007. Determination of size and concentration of gold nanoparticles from UV−Vis spectra. Analytical Chemistry, 79(11), 4215–4221.
9. Hua, Z., Yu, T., Liu, D., Xianyu, Y. 2021. Recent advances in gold nanoparticles-based biosensors for food safety detection. Biosensors and Bioelectronics, 179, 113076. https://doi.org/https://doi.org/10.1016/j.bios.2021.113076
10. Iqbal, M., Usanase, G., Oulmi, K., Aberkane, F., Bendaikha, T., Fessi, H., Zine, N., Agusti, G., Errachid, E.S., Elaissari, A. 2016. Preparation of gold nanoparticles and determination of their particles size via different methods. Materials Research Bulletin, 79, 97–104. https://doi.org/10.1016/j.materresbull.2015.12.026
11. Issa, A., Aqel, M. O.A., Zakout, B., Daqqa, A.A., Amassi, M., Naim, N. 2019. 5-DOF robot manipulator modelling, development and automation using LabVIEW, Vision Assistant, and Arduino. International Conference on Promising Electronic Technologies (ICPET), 124–129. https://doi.org/10.1109/ICPET.2019.00030
12. Korgin, A., Ermakov, V., Kilani, L.Z. 2019. Automation and Processing Test Data with LabVIEW Software. IOP Conference Series: Materials Science and Engineering, 661(1), 12073. https://doi.org/10.1088/1757-899X/661/1/012073
13. Kumari, S., Singh, V., Singh, D. 2024. Nanoparticle synthesis advancements and their application in wastewater treatment: A comprehensive review. Current Chemistry Letters, 13(1), 31–40. https://doi.org/10.5267/j.ccl.2023.9.002
14. Liu, X.Y., Wang, J.Q., Ashby, C.R., Zeng, L., Fan, Y.F., Chen, Z.S. 2021. Gold nanoparticles:

synthesis, physiochemical properties and therapeutic applications in cancer. Drug Discovery Today, 26(5), 1284–1292. https://doi.org/https://doi.org/10.1016/j.drudis.2021.01.030

15. Mohandas, N. 2020. A nano-tale of the vivid colours of gold. https://researchmatters.in/sciqs/nano-tale-vivid-colours-gold
16. Montalvan, L.T., Jordan, E., Tubón, E., Carrillo, S., Heredia, E., Salazar, F. 2022. Smart control and monitoring system of a robotic station operating with motion control and artificial vision. RISTI - Revista Iberica de Sistemas e Tecnologias de Informacao, 2022(E49), 222–236. https://www.scopus.com/inward/record.uri?eid=2-s2.0-85136284758&partnerID=40&md5=fb97abb4c752a4d899df76ef39d51007
17. Nag, O.K., Muroski, M.E., Hastman, D.A., Almeida, B., Medintz, I.L., Huston, A.L., Delehanty, J.B. 2020. Nanoparticle-mediated visualization and control of cellular membrane potential: Strategies, progress, and remaining issues. ACS Nano, 14(3), 2659–2677. https://doi.org/10.1021/acsnano.9b10163
18. NI. 2023. Using the Vision Assistant Express VI - NI. https://www.ni.com/docs/en-US/bundle/ni-vision-assistant-help/page/expressvi_howto.html
19. Ordoñez-Avila, J.L., Maldonado, E.R.T., Magomedov, I. 2022. Water generation based on condensation controlled by gray scale and artificial vision. International Conference on Information, Control, and Communication Technologies (ICCT), 1–5. https://doi.org/10.1109/ICCT56057.2022.9976774
20. Paramasivam, G., Sanmugam, A., Palem, V.V, Sevanan, M., Sairam, A.B., Nachiappan, N., Youn, B., Lee, J.S., Nallal, M., Park, K.H. 2024. Nanomaterials for detection of biomolecules and delivering therapeutic agents in theragnosis: A review. International Journal of Biological Macromolecules, 254. https://doi.org/10.1016/j.ijbiomac.2023.127904
21. Quantel. 2019. Q-smart 450 Pulsed Nd:YAG Laser, 213 to 1064 nm, 8 to 450 mJ, product - photonic solutions, UK. https://www.photonicsolutions.co.uk/product-detail.php?prod=6345
22. Serafino, S.E., Cicerchia, L.B., Pérez, G., Adorno, S., Balmer, A. 2020. Detection and counting of lemons using artificial vision and tracking techniques for real time harvest estimation. XLVI Latin American Computing Conference (CLEI), 496–502. https://doi.org/10.1109/CLEI52000.2020.00064
23. Sivaranjani, S., Velmurugan, S., Kathiresan, K., Karthik, M., Gunapriya, B., Gokul, C., Suresh, M. 2021. Visualization of virtual environment through LabVIEW platform. Materials Today: Proceedings, 45, 2306–2312. https://doi.org/https://doi.org/10.1016/j.matpr.2020.10.559
24. Strem Chemicals. 2011. Spherical Gold Nanoparticles Kit (30-90 nm). https://www.azonano.com/article.aspx?ArticleID=2875
25. Torrisi, L., Cutroneo, M., Torrisi, A., Di Marco, G., Fazio, B., Silipigni, L. 2020. IR ns pulsed laser irradiation of Polydimethylsiloxane in vacuum. Vacuum, 177, 109361. https://doi.org/https://doi.org/10.1016/j.vacuum.2020.109361
26. Torskal Nanoscience, 2022. Standard gold nanoparticles introduction. https://www.torskal.com/product/standard-gold-nanoparticles-introduction-pack/
27. Weichelt, R., Ye, J., Banin, U., Eychmüller, A., Seidel, R. 2019. DNA-mediated self-assembly and metallization of semiconductor nanorods for the fabrication of nanoelectronic interfaces. Chemistry - A European Journal, 25(38), 9012–9016. https://doi.org/10.1002/chem.201902148
28. Wisultschew, C., Otero, A., Portilla, J., Torre, E. 2019. Artificial vision on edge IoT devices: a practical case for 3D data classification. XXXIV Conference on Design of Circuits and Integrated Systems (DCIS), 1–7. https://doi.org/10.1109/DCIS201949030.2019.8959857
29. Zhang, Y., Li, Y., Gu, X., Liu, H., Zhang, Y., Hu, W. 2019. Laser spot image acquisition and processing based on LabVIEW. Optik, 185, 505–509. https://doi.org/https://doi.org/10.1016/j.ijleo.2018.12.051
30. Zhou, Z., Li, J., Yuan, Y., Gao, L., He, P., Luo, G., Xie, Y., Zhang, J., Xu, G., Liao, X., Zhang, S. 2023. Size controlled, structural characterization and applications of glucopyranoside-based N-heterocyclic carbenes stabilized gold nanoparticles. Journal of Molecular Liquids, 386. https://doi.org/10.1016/j.molliq.2023.122543